

# Experimental observation of spectral gap in microwave $n$ -disk systems

S. Barkhofen,<sup>1</sup> T. Weich,<sup>1,2</sup> A. Potzuweit,<sup>1</sup> H.-J. Stöckmann,<sup>1</sup> U. Kuhl,<sup>3,1</sup> and M. Zworski<sup>4</sup>

<sup>1</sup>*Fachbereich Physik, Philipps-Universität Marburg, Renthof 5, 35032 Marburg, Germany*

<sup>2</sup>*Fachbereich Mathematik, Philipps-Universität Marburg, Hans-Meerwein-Str., 35032 Marburg, Germany*

<sup>3</sup>*Laboratoire de Physique de la Matière Condensée, CNRS UMR 7336,*

*Université de Nice Sophia-Antipolis, F-06108 Nice, France\**

<sup>4</sup>*Department of Mathematics, University of California, Berkeley, California 94720, USA*

(Dated: December 27, 2012)

We present experimental studies of the symmetry reduced three-disk and five-disk systems using a microwave setup. By extracting the complex resonances from the signal by means of the method of the harmonic inversion we can access the distribution of the imaginary parts or the width distribution. While increasing the opening of the systems, a spectral gap is observed for thick as well as for thin repellers and for the latter case it is compared with the known topological pressure bounds. Furthermore the maxima of the distributions are found to coincide for a large range of the distance to radius parameter with half of the classical escape rate. These results confirm theoretical predictions based on rigorous mathematical analysis in the case of the spectral gap and on numerical experiments in the case of the maxima of the distributions.

PACS numbers: 05.45.Mt, 03.65.Nk, 42.25.Bs, 25.70.Ef

Keywords: Spectral Gap, Weyl law, fractal repeller,  $n$ -disk system, harmonic inversion

In semiclassical physics one is interested in the relation between quantities from classical mechanics and from quantum mechanics asymptotically for small *effective* Planck constant of the system. Two manifestations of the classical quantum correspondence for closed systems are the Weyl law [1] and the Gutzwiller [2, 3] trace formula. The Weyl law describes asymptotically the number of quantum mechanical energy levels in terms of the classical phase space dimension. The trace formula describes the fluctuations of the density of states around the Weyl law by means of classical periodic orbits and their stability [3].

For open systems there are also results connecting classical and quantum quantities [4, 5]. Their derivation is however much more delicate because the classical energy shells in phase space become non compact and the real valued eigenvalues of the Hamiltonian are replaced by complex resonances [6–8]. For open systems the imaginary parts of resonances are always negative and they correspond to the rate of decay of the corresponding unstable states.

A celebrated example of a semiclassical formula is the fractal Weyl law for open chaotic systems with fractal repeller. It gives the asymptotic behavior of the counting function, that is the number of resonances up to some energy, for a fixed bound of the imaginary part. There exists numerous mathematical [9, 10], numerical [11–14] and experimental [15–17] studies during the last years. Another line of research focuses on the distribution of the imaginary parts in the semiclassical limit [14].

A paradigmatic open system with a classical fractal repeller is the  $n$ -disk system (see Fig. 1). It has been introduced in the late 80s by Ikawa in mathematics [18]

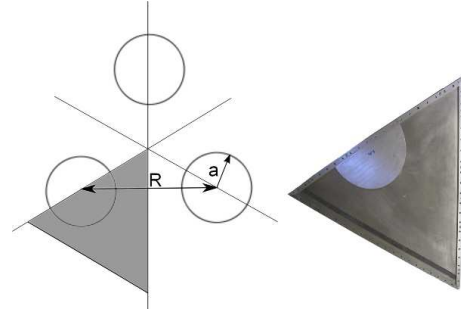


FIG. 1. (Color online) Left: Sketch of three-disk system, where one fundamental domain is shaded. Right: Photograph of the experimental cavity without top plate including the disk inset and the absorber.

and by Gaspard, Rice [19, 20] and Cvitanović, Eckhardt [21] in physics. A  $n$ -disk system describes the scattering of a classical or quantum mechanical particle in a two-dimensional plane on  $n$  hard disks whose centers form a regular polygon. The distance between the centers is historically denoted by  $R$  and the disk radius by  $a$ . Up to scaling the geometry is completely defined by the ratio  $R/a$  (see Fig. 1).

The quantum system is described by the Helmholtz equation

$$-\nabla^2 \psi_n = k_n^2 \psi_n \quad (1)$$

with Dirichlet boundary conditions at the disks boundary. As the system is open the quantum resonances  $k_n = \text{Re } k_n + i \text{Im } k_n$  are complex valued. For the three-disk system Gaspard and Rice [22] gave an explicit expression for the scattering matrix in terms of Bessel and Hankel functions which allows to calculate the quantum resonances numerically.

Classically one studies the trajectories of particles

\* ulrich.kuhl@unice.fr

which perform hard wall reflections on the disks. From periodic trajectories a wide range of classical quantities like the classical escape rate, the fractal dimension of the repeller and the topological pressure can be calculated using the classical Ruelle  $\zeta$ -function [20],

$$\zeta_\beta(z) = \prod_p \left[ 1 - \frac{\exp(-zT_p)}{\Lambda_p^\beta} \right]^{-1} \quad (2)$$

where the product runs over the primitive periodic orbits,  $T_p$  are the corresponding period lengths and  $\Lambda_p$  the stabilities. The topological pressure  $P(\beta)$  is then defined as the smallest real pole of  $\zeta_\beta(z)$ . An effective way of its calculation is the cycle expansion, introduced by Cvitanović and Eckhardt [21, 23]. The classical escape rate is given by  $\gamma = -P(1)$  and the reduced Hausdorff dimension  $d_H$  of the fractal repeller by the Bowen pressure formula  $P(d_H) = 0$  [24].

In 1988 and 1989 Ikawa and Gaspard-Rice independently derived a connection between the topological pressure, being a purely classical quantity, and the quantum mechanical spectral gap. A spectral gap in this context is a constant  $C < 0$  such that  $\text{Im } k_n \leq C$ . Gaspard and Rice started from Gutzwiller's trace formula and used semiclassical zeta functions to conclude that  $\text{Im } k_n \leq P(1/2)$ . They also confirmed this estimate numerically [19]. Later this estimates for the spectral gap has been also obtained mathematically for more general semiclassical systems [25]. It is, however, known that this bound is in general not optimal as it does not take into account phase cancellation (see section 8.2 in [5] and [26]). Especially for weakly open systems this bound has no implication: As  $P(\beta)$  is monotonously decreasing it is evident that for systems with  $d_H > 1/2$  the bound  $P(1/2)$  is positive, but the imaginary parts are negative anyway. Such systems are nowadays also called systems with “thick repeller” in contrast to systems with “thin repeller” where  $d_H < 1/2$  and  $P(1/2)$  is a true constraint on the imaginary parts (see e.g. [5]).

The same estimate on the spectral gap has been obtained in the 70s by Patterson and Sullivan [27, 28] for scattering on hyperbolic quotients  $\Gamma \backslash \mathbf{H}^2$  of infinite volume which provide a mathematical model for chaotic scattering [29]. In that case, quantum resonances (defined as poles of the scattering matrix of the surface) coincide with the zeros of the Selberg zeta function and the topological pressure can be calculated explicitly using  $\delta$ , the dimension of the limit set of  $\Gamma$ :  $P(\beta) = \delta - \beta$ . Results of [27, 28] imply, that all resonances satisfy  $\text{Im } k \leq \delta - 1/2$ . For this model the estimate is known to be sharp as there always exists a resonance at  $i(\delta - 1/2)$  (corresponding to a bound state when  $\delta - 1/2 > 0$ ). However, there are no other resonances for  $\text{Im } k < P(1/2) - \epsilon$ , for some small  $\epsilon > 0$  [30]. The question of further improvements for the spectral gap is an active field of mathematical research with deep applications to number theory [5, 31].

Another interesting property of the  $\text{Im } k$ -distribution

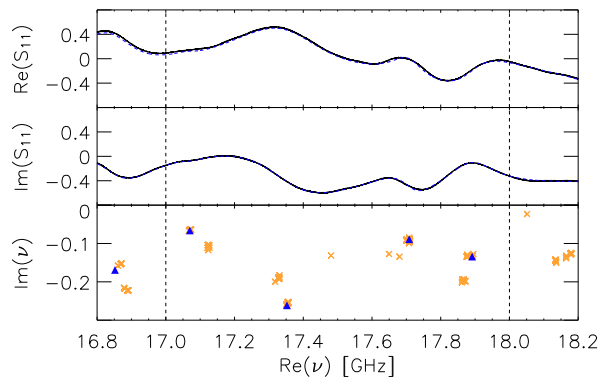


FIG. 2. (Color online) Three-disk system at  $R/a = 2.88$ : in the lowest panel resonances belonging to good (orange crosses) and the best reconstruction (blue triangles) are shown in the complex plane within a small frequency range, the upper 2 panels include the measured signal (black, dashed) and best reconstruction (blue) in this window (vertical lines) based on the poles marked by the blue triangles, presented in real and imaginary part

has been observed in [13]: The imaginary parts of numerically calculated resonances were found to concentrate at  $\text{Im } k = -\gamma_{\text{cl}}/2 = P(1)/2$  that is at the half of the classical escape rate. This corresponds to the classical expectation as the quantum mechanical probability density is the modulus square of the wave function [19]. Although no mathematical result supports the claim that imaginary parts of resonances concentrate at  $-\gamma_{\text{cl}}/2$ , Naud [32] has shown that the density of resonances for  $\text{Im } k > -\gamma_{\text{cl}}/2$  is *lower* than the prediction from the fractal Weyl law [33–35].

Another connection between the classical escape rate and the quantum spectrum has been experimentally observed in microwave studies of  $n$ -disk systems [15, 16]: Lu et al observed that the decay of the wave-vector autocorrelation function for small wave vectors is related to the classical escape rate [15].

In this Letter we will focus on the spectral gap and the maximum of the experimentally obtained  $\text{Im } k$ -distribution and compare them to the calculated topological pressure and the classical escape rate, respectively. We would like to note that all following investigations were performed in the low lying  $k$ -regime.

In order to simplify the  $n$ -disk systems we exploit their  $D_n$  symmetry and study the symmetry reduced systems. In the reduction to the fundamental domain also the two enclosing symmetry axes are hard wall potentials acting as “mirrors” (see shaded area in Fig. 1). For the quantum mechanical system the Dirichlet boundary condition at the symmetry axes imply that the corresponding scattering resonances belong to the  $A_2$  representation.

In the experiments we realized the quantum version of the symmetry reduced three- and five-disk system using a microwave cavity. The triangular resonator (Fig. 1) has two metallic side walls of length 100 cm including an angle of  $60^\circ$  for the three-disk, and  $36^\circ$  for the five-disk

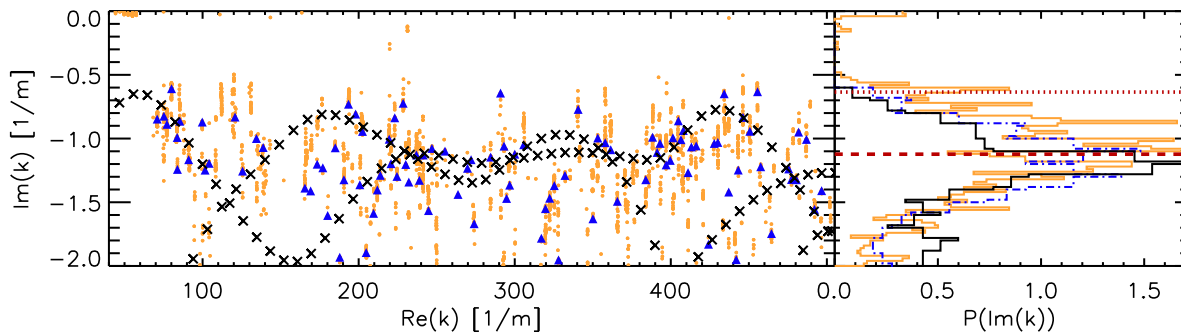


FIG. 3. (Color online) In the left panel the resonances for  $R/a = 5.5$  in the complex  $k$ -plane are shown as well as the distribution of the imaginary parts of  $k$  in the right panel. The shown  $k$  range corresponds to a frequency range from 2 to 24 GHz. The orange clouds correspond to all resonances leading to good reconstruction as well as the orange histogram. Note that many orange dots might overlay each other. Blue triangles and blue dashed-dotted histogram describe the set belonging to the best reconstruction. Black crosses are the numerically calculated poles and the solid black histogram the corresponding distribution. The dotted red line in the right panel is  $P(1/2)$ , the red dashed line  $-\gamma_{cl}/2$ .

system, respectively, and the third side covered with absorbers avoiding reflections at the open end. The  $R/a$  parameter can be changed by moving a half-disk inset of radius  $a = 19.5$  cm, which is in contact with top and bottom plate, along the side wall. In the three-disk system the  $R/a$  range between 2.26 and 6.17 was technically accessible, in the five-disk case we were able to measure between 2 and 3.9. The half-disk inset was moved in steps of 10 mm. A short wire antenna ( $r=0.7$  mm) is inserted through a hole in the top plate, placed in the interior region, and it is sufficiently short not to touch the bottom plate. The height of the cavity  $h = 6$  mm leads to a cutoff frequency of 25 GHz. Within the frequency range from 2 to 24 GHz only the  $TM_0$  mode can propagate and the cavity may be considered as two-dimensional. Hence the equivalence between wave mechanics and quantum mechanics, i.e. between the time independent Helmholtz and Schrödinger equation, exists (for details of the experimental setup see [17], for a general introduction to microwave billiards see chapter 2.2 in [36]).

A vector-network-analyzer (VNA) is used for measuring and reveals the complex  $S$ -matrix. Under the assumption of a point-like antenna the measured reflection signal equals [37]

$$S_{11}(\nu) = 1 + \sum_j \frac{\tilde{A}_j}{\nu^2 - \nu_j^2} \quad (3)$$

where  $\nu_j$  are the complex valued resonance positions. The extraction of  $\nu_j$  and  $\tilde{A}_j$  from the signal is the task of the data analysis: For closed systems and low frequencies the resonances are well separated and could be treated by a multi-Lorentz-fit. But for open systems, where the resonances overlap strongly, a fit would not converge. Therefore we applied the harmonic inversion (HI) [38–40] on the signal, a sophisticated nonlinear algorithm, to extract complex poles from the measured signals. To guarantee an equal treatment we used it for all measurements. The HI was already used to analyze ex-

perimental line widths in the presence of wall absorption and additional open channels [40] and to study the fractal Weyl law [17]. In the latter our way of using the HI was already discussed in detail, thus we state here only the main ideas: For non-ideal, i.e. experimental, data we have shown that the HI should be applied several times with different sets of its internal parameters, any leading to a set of complex poles and amplitudes. Afterwards the reconstruction based on these results is compared to the original signal. Fig. 2 shows part of a typical spectrum (black solid line) and the best (concerning the  $\chi^2$ -error) individual reconstruction (blue dashed line) within the window indicated by the vertical lines. The corresponding resonances are marked by blue triangles in the lower panel, the complex plane. The orange crosses belong to other resonance sets, also leading to good reconstructions (to maintain clarity they are not shown in the upper two panels), called *good resonances*. Other sets not meeting the criterion are rejected for further analysis.

For the three-disk system we checked the reliability of the HI by comparing the experimental resonances with calculations based on the algorithm of Gaspard and Rice [22]. However even for experiments with closed microwave systems it is known that only the lowest lying resonances agree well with the theoretical predictions. For higher frequencies the experimental perturbations disturb the measured spectrum such that the measured resonances cannot be associated directly to the theoretical ones, but statistical properties such as the resonance density persist. For an open system we expect this effect to be even more significant as the spectra of non hermitian Hamiltonians are known to be much more unstable under perturbations compared to hermitian Hamiltonians [41].

Fig. 3 shows again the good HI-resonances in orange and the best in blue for  $R/a = 5.5$  and in the full measured  $Re k$ -range from 40 to 500  $m^{-1}$ . Again the orange poles form "clouds" around the blue triangles – the elongated shape of the clouds is a consequence of

the non-isometric axis ranges. The black crosses indicate the numerically calculated resonances. The composition of resonance chains is typical for large  $R/a$  parameters [13, 22, 42]. The individual resonances are not reproduced by the experimental data due to inevitable reflections at the absorbers and the perturbation by the antenna but the resonance free regions and the resonance density coincide.

In the right part of Fig. 3 the corresponding  $\text{Im } k$  distributions  $P(\text{Im } k)$  are shown, in solid black for the numerically calculated and in dashed-dotted blue for the experimental spectrum. Both distributions show up to be the same within the limits of error. The same was true for all good reconstructions passing the  $\chi^2$  criterion. All  $P(\text{Im } k)$  distributions shown below have hence obtained by superimposing the results of all good reconstructions. One example is shown in the right hand part of Fig. 3 in orange. In fact one can show that  $P(\text{Im } k)$  is robust with respect to errors in the reconstruction as long as the number of resonances entering the reconstruction is approximately the same. For the example shown in Fig. 3 the number varied between 94 for the numerical data and 117 for the individual reconstruction.

By measuring the averaged  $\text{Im } k$  distribution for symmetry reduced three- and five-disk systems for different  $R/a$  parameters we can now study the dependence of the  $\text{Im } k$  distribution on the opening of the system (Fig. 4). For every  $R/a$  value the averaged histogram of the  $\text{Im } k$  distribution is plotted as a shade plot. For the five-disk case the measured data is presented in Fig. 4(a). For  $R/a = 2$  the system is completely closed however we observe already a small gap  $\approx 0.15 \text{ m}^{-1}$  caused by antenna and wall absorbing effects. While opening the system the very narrow  $\text{Im } k$  distribution first gets wider and the maximum of the distribution moves towards higher imaginary parts. From  $R/a \approx 2.5$  the resonance free region starts to grow and reaches a value of  $\approx 0.5 \text{ m}^{-1}$  for the maximal accessible opening at  $R/a = 3.9$ . Over the whole  $R/a$  range the value of  $P(1/2)$  stays positive, thus providing no lower bound on the spectral gap. The solid black line in the shade plot shows half the classical escape rate calculated by the cycle expansion. We show this curve down to  $R/a = 2.41$ , because for lower  $R/a$  values so called pruning sets in (for orbits up to order 4): Due to those periodic orbits which are destroyed when the disks are too close the symbolic dynamic is not complete anymore -which was fundamental in the cycle expansion [21]. In accordance with calculations in the high frequency regime [13] our experiment in a much lower frequency regime shows that the maximum of the  $\text{Im } k$  distribution is described by  $-\gamma_{\text{cl}}/2$ . We emphasize that there are no free parameters to fit  $\gamma_{\text{cl}}$  to the experiments.

A more open systems is the three-disk system. Here the repeller becomes thin for  $R/a \geq 2.83$ , i.e.  $P(1/2)$  provides a lower bound on the gap. Again one observes that the gap first increases and only for high  $R/a$  values coincides with the lower bound  $P(1/2)$  (dotted black line). At which  $R/a$  value exactly the gap in the ex-

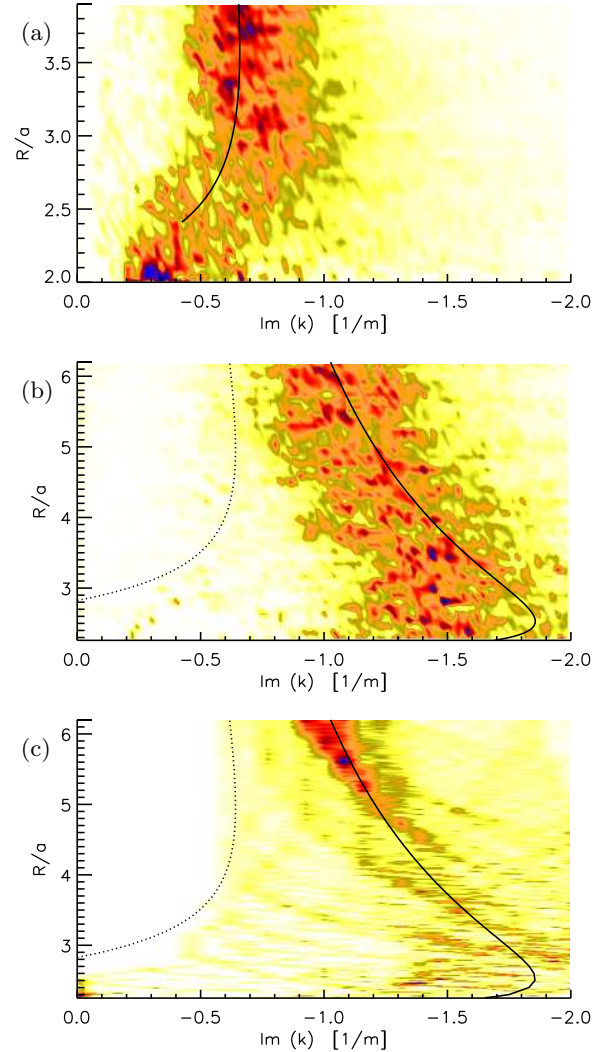


FIG. 4. (Color online) Shade plots of the distribution of  $\text{Im } k$  using a color code from white to dark blue for (a) the five-disk experiment, (b) the three-disk experiment, and (c) the three-disk simulation as a function of the  $R/a$  parameter. The classical escape rate (precisely:  $-\gamma_{\text{cl}}/2$ ) is the solid black line.  $P(1/2)$  corresponds to the dotted line. For the five-disk case the  $P(1/2)$  is still positive and hence does not arise in the plot.

periment opens and whether it opens before  $P(1/2)$  becomes negative is less clear as in the five-disk system. The area of the totally closed system ( $R/a = 2$ ) is too small to enable meaningful measurements. Since there are no pruned orbits until order 4 from  $R/a = 2.01$ , we are able to plot the calculated curve for the full measured range. The maximum of the  $\text{Im } k$  distribution decreases for  $R/a > 3$  which might be surprising at first sight. The reason is that the time of flight between two scattering events increases linearly which will overcompensate the defocussing effect of a scattering event for large enough  $R/a$ . This leads to the decrease of  $-\gamma_{\text{cl}}/2$  (solid black



line), following the maximum of the distribution.

As a consistency check Fig. 4(c) shows the shade plot for the numerical data of the symmetry reduced three-disk system. Also there the correspondence of  $-\gamma_{cl}/2$  (solid black line) is clearly visible only for large and less prominent for smaller  $R/a$  values. For large  $R/a$  the lower bound  $P(1/2)$  (dotted black line) coincides well with the numerically observed gap. The opening of it however is not described by  $P(1/2)$  which becomes obvious for  $2.5 < R/a < 2.83$ . Here  $P(1/2)$  is still positive but a clear gap is already visible, the same phenomenon as observed in the experimental data of the five-disk system.

In this Letter we have demonstrated the existence of a spectral gap in open chaotic  $n$ -disk microwave systems. We could extract the resonances from the measured signal and thus had direct access to the gap and the maximum of the  $\text{Im } k$  distribution. These were compared

with the calculated classical values for  $P(1/2)$  and  $\gamma_{cl}/2$ . A good agreement was found for sufficiently open systems. But we could also show that the bound  $P(1/2)$  does not describe the opening range of neither the experimental nor the exact quantum mechanically calculated data. We would like to emphasize that all investigations were performed in the low lying  $k$  regime thus showing a remarkable agreement with the semiclassical predictions.

We are grateful to S. Nonnenmacher and B. Eckhardt for intensive discussions, and to S. Möckel for providing the code for the calculation of the quantum mechanical resonances. This work was supported by the Deutsche Forschungsgemeinschaft via an individual grant and the Forschergruppe 760 ‘Scattering systems with complex dynamics’. TW acknowledges financial support by the ‘German National Academic Foundation’, UK the support by the CNRS-INP via the programm PEPS-PTI, and MZ by the NSF via the grant DMS-1201417.

- 
- [1] H. Weyl, Math. Annalen, **71**, 441 (1912).
  - [2] M. C. Gutzwiller, J. Math. Phys., **12**, 343 (1971).
  - [3] M. C. Gutzwiller, *Chaos in Classical and Quantum Mechanics*, Interdisciplinary Applied Mathematics, Vol. 1 (Springer, New York, 1990).
  - [4] E.-M. Graefe, M. Höning, and H. J. Korsch, J. Phys. A, **43**, 075306 (2010).
  - [5] S. Nonnenmacher, Nonlinearity, **24**, R123 (2011).
  - [6] N. Moiseyev, Phys. Rev., **302**, 211 (1998), ISSN 0370-1573.
  - [7] M. Zworski, Not. AMS, **43**, 319 (1999).
  - [8] U. Kuhl, O. Legrand, and F. Mortessagne, Fortschritte der Physik, **61** (2013), doi:10.1002/prop.201200101.
  - [9] J. Sjöstrand, Duke Math. J., **60**, 1 (1990).
  - [10] J. Sjöstrand and M. Zworski, Duke Math. J., **137**, 381 (2007).
  - [11] H. Schomerus, K. M. Frahm, M. Patra, and C. W. J. Beenakker, Physica A, **278**, 469 (2000).
  - [12] K. K. Lin, J. Comp. Phys., **176**, 295 (2002).
  - [13] W. T. Lu, S. Sridhar, and M. Zworski, Phys. Rev. Lett., **91**, 154101 (2003).
  - [14] H. Schomerus, J. Wiersig, and J. Main, Phys. Rev. A, **79**, 053806 (2009).
  - [15] W. Lu, M. Rose, K. Pance, and S. Sridhar, Phys. Rev. Lett., **82**, 5233 (1999).
  - [16] W. Lu, L. Viola, K. Pance, M. Rose, and S. Sridhar, Phys. Rev. E, **61**, 3652 (2000).
  - [17] A. Potzuweit, T. Weich, S. Barkhofen, U. Kuhl, H.-J. Stöckmann, and M. Zworski, Phys. Rev. E, **86**, 066205 (2012).
  - [18] M. Ikawa, Ann. Inst. Fourier, **38**, 113 (1988).
  - [19] P. Gaspard and S. A. Rice, J. Chem. Phys., **90**, 2242 (1989).
  - [20] P. Gaspard and S. A. Rice, J. Chem. Phys., **90**, 2225 (1989).
  - [21] P. Cvitanović and B. Eckhardt, Phys. Rev. Lett., **63**, 823 (1989).
  - [22] P. Gaspard and S. A. Rice, J. Chem. Phys., **90**, 2255 (1989).
  - [23] B. Eckhardt, G. Russberg, P. Cvitanović, P. Rosenqvist, and P. Scherer, in *Quantum Chaos Between Order and Disorder*, edited by C. Casati and B. Chirikov (University Press, Cambridge, 1995) p. 405.
  - [24] R. Bowen, Inst. Hautes Études Sci. Publ. Math., **50**, 1 (1979).
  - [25] S. Nonnenmacher and M. Zworski, Acta Mathematica, **203**, 149 (2009).
  - [26] V. Petkov and L. Stoyanov, Anal. PDE, **3**, 427 (2010).
  - [27] S. J. Patterson, Acta Mathematica, **136**, 241 (1976).
  - [28] D. Sullivan, Inst. Hautes Études Sci. Publ. Math., **50**, 171 (1979).
  - [29] D. Borthwick, *Spectral Theory of Infinite-Area Hyperbolic Surfaces*, Progress in Mathematics, Vol. 256 (Birkhäuser, Boston, 2007).
  - [30] F. Naud, Ann. Sci. Ecole Norm. Sup., **38**, 116 (2005).
  - [31] J. Bourgain, A. Gamburd, and P. Sarnak, Acta Mathematica, **207**, 255 (2011).
  - [32] F. Naud, “Density and localization of resonances for convex co-compact hyperbolic surfaces,” Preprint (2011), arXiv:1203.4378.
  - [33] L. Guillopé, K. K. Lin, and M. Zworski, Commun. Math. Phys., **245**, 149 (2004).
  - [34] M. Zworski, Inventiones mathematicae, **136**, 353 (1999).
  - [35] K. Datchev and S. Dyatlov, “Fractal weyl laws for asymptotically hyperbolic manifolds,” Preprint (2012), arXiv:1206.2255v3.
  - [36] H.-J. Stöckmann, *Quantum Chaos - An Introduction* (University Press, Cambridge, 1999).
  - [37] J. Stein, H.-J. Stöckmann, and U. Stöckmann, Phys. Rev. Lett., **75**, 53 (1995).
  - [38] J. Main, Phys. Rep., **316**, 233 (1999).
  - [39] J. Main, P. A. Dando, D. Belkić, and H. S. Taylor, J. Phys. A, **33**, 1247 (2000).
  - [40] U. Kuhl, R. Höhmann, J. Main, and H.-J. Stöckmann, Phys. Rev. Lett., **100**, 254101 (2008).
  - [41] L. N. Trefethen and M. Embree, *Spectra and Pseudospectra: The Behavior of Nonnormal Matrices and Operators* (Princeton University Press, Princeton, New Jersey, USA, 2005).
  - [42] A. Wirzba, Phys. Rep., **309**, 1 (1999).